



CrossMark
click for updates

Cite this: *RSC Adv.*, 2015, 5, 65913

Amino acid functionalized blue and phosphorous-doped green fluorescent carbon dots as bioimaging probe†

Saheli Sarkar, Krishnendu Das, Moumita Ghosh and Prasanta Kumar Das*

Amino acid functionalized carbon dots (CDs) were synthesized in a simple and cost effective bottom up approach. Citric acid was used as the source of the carbon core and three amino acids L-isoleucine, L-valine and glycine were used for the surface fabrication of CDs to produce CD_{iso}, CD_{val} and CD_{gly}, respectively. Interestingly these CDs were found to fluoresce with a blue emission. Doping of phosphorus to these CDs (PCDs) tuned the photoemission properties and produced green emitting PCDs. The doping of phosphorous (P) to these CDs improved their fluorescence intensity as well as quantum yields. Both doped and non-doped CDs were characterized by spectroscopic and microscopic techniques. These highly stable CDs were biocompatible in nature and did not exhibit any photobleaching property over a long span of time even under UV exposure. Subsequently, these CDs were exploited as an excellent bioimaging probe. Importantly CDs and PCDs illuminated cells in two completely different spectral regions blue and green, respectively in accordance with their fluorescence spectral behaviour. Hence, amino acid functionalized carbon dots based bioimaging probes with different fluorescence characteristics were developed that are widely applicable for cellular imaging in both blue and green spectral regions.

Received 26th May 2015

Accepted 28th July 2015

DOI: 10.1039/c5ra09905f

www.rsc.org/advances

1. Introduction

Fluorescent carbon dots (CDs) represent a fascinating class of 'zero-dimensional' carbon nanomaterials that comprise of discrete, spherical nanoparticles with size less than 10 nm.¹⁻⁴ These CDs have high potential to be used in energy storage, bioimaging, drug delivery, sensors, and diagnostics.⁴⁻¹¹ CDs have attracted extensive attention due to their outstanding advantages such as stable photoluminescence properties, high aqueous solubility, versatile surface chemistry and low toxicity compared to environmentally hazardous and toxic nanomaterials including lead, cadmium *etc.*^{5,12} The other frequently used semiconductor based quantum dots like CdS, CdSe, PbSe are composed of toxic heavy metals and suffer from cytotoxicity, low aqueous solubility that restrict their application in bioimaging.¹³ Fluorescent CDs, tiny light emitting particles on nanometer scale, are gaining importance in cellular imaging over conventional organic dyes and fluorescent proteins because of improved signal brightness,

resistance against photobleaching, size dependent fluorescence emission, and simultaneous excitation of multiple fluorescence colours.^{14,15}

To date, two distinct methods have been explored for carbon dot synthesis namely the top down and bottom up approach.⁵ In the top-down approach, graphite and its derivatives are used to synthesize CDs through laser ablation, arc discharge and electrochemical oxidation.^{3,5,16-20} Alternatively, in bottom-up approach, solvothermal methods, pyrolysis, microwave treatment, ultrasonic-assisted synthetic procedures are exploited to synthesize CDs from carbonaceous organic molecules.²¹⁻²⁶ In general, due to their simple and cost effective approach, bottom-up is more favourable than that of top-down techniques. Candle soot, carbohydrate, polyhydric alcohol, polyhydric acid, orange juice, strawberry juice, cucumber juice are some of the well known carbon precursors to synthesize CDs.^{2,14,27-30} To this end, amino acid (primarily histidine) also has been used for preparing fluorescent CDs.⁵ Jiang, *et al.* has reported the photoluminescence of CDs derived from hydrophilic amino acids while hydrophobic amino acids showed weak fluorescence.¹ Also synthetic method and chemical composition has a significant effect on emission property of CDs. The emission of CDs has been modified by varying the reaction temperature, nature of solvent, capping ligands, and surface functionalizing agents.³¹⁻³³ Doping is another important tool for varying spectral behaviour of CDs. Phosphorous, nitrogen, sulphur, boron have been doped to tune the quantum

Department of Biological Chemistry, Indian Association for the Cultivation of Science, Jadavpur, Kolkata - 700 032, India. E-mail: bcpkd@iacs.res.in

† Electronic supplementary information (ESI) available: IR spectra of CDs and PCDs, NMR spectra of CDs and PCDs, table for zeta potential values of CDs and PCDs, XRD pattern of CD_{val} and PCD_{val}, XPS pattern of CD_{val} and PCD_{val}, EDX analysis, excitation wavelength dependent emission of CD_{gly} and PCD_{gly}, photostability of CDs and PCDs under UV light irradiation. See DOI: 10.1039/c5ra09905f

yield of CDs and change its emission properties.^{16,32,34} Hydrophilic and hydrophobic surface functionalization have also been employed to tune the emission behaviour of CDs.³³ Interestingly, though amino acids have been used as precursor for the synthesis of CDs, but they have been very little explored for surface functionalization of CDs. In this regard, recently we reported the synthesis of cationic and anionic surface functionalized fluorescent CDs from very simple precursor glycine, Tris, and citric acid and subsequently they have been used for histone sensing and enzyme probing.^{9,35} Thus, the need of simple methods for developing CDs and their surface functionalization is highly demanding considering its potential applications in biomedicine. However, less attention has been given to tune the emission properties of CDs by varying surface functionalization. To this end, use of amino acid for surface functionalization of CDs as well as doping of phosphorous to tune the spectral behaviour of these amino acid functionalized CDs and subsequently their application in bioimaging has not yet been investigated.

Previously reported CDs derived from hydrophobic amino acids including L-isoleucine, L-valine showed poor water solubility and weak fluorescence.¹ Herein we report the synthesis of highly fluorescent CDs using citric acid as the carbon core³⁶ and surface functionalization with naturally occurring hydrophobic amino acids. Highly water soluble fluorescent CDs were functionalized with three different aliphatic amino acids glycine, L-valine and L-isoleucine. Interestingly these CDs were found to be blue emitting. Their photoemission properties as well as the quantum yields were subsequently tuned by doping phosphorous (P), which increased their fluorescence intensity as well as quantum yields. More importantly P-doping changed the photoemission properties of all three CDs exhibiting green emission. These P-doped and non-doped CDs were characterized by spectroscopic and microscopic techniques. The aqueous suspension of both P-doped and non-doped CDs were highly stable for long time and resistant towards photo bleaching effect even under UV exposure. The aqueous suspension of these P-doped and non-doped fluorescent CDs were biocompatible up to 800 $\mu\text{g mL}^{-1}$. The photoemission behaviour of these non-doped and P-doped CDs in two completely different spectral regions (blue and green) was utilized as bioimaging probe.

2. Materials and methods

2.1. Materials

Glycine, L-valine, L-isoleucine were purchased from SRL (India) and citric acid was procured from Spectrochem (India). Milli-Q water was used throughout the study. The UV-vis absorption spectra were recorded on a PerkinElmer Lambda 25 spectrophotometer. Fluorescence spectra were recorded in Varian Cary Eclipse luminescence spectrometer. Lyophilization was done in a Virtis 4KBTXL-75 freeze-drier. Thermo Scientific Espresso centrifuge was used for centrifugation, and zeta potential was measured in a zetasizer Nano-ZS of Malvern Instruments Limited. ¹H NMR spectra were recorded on a Bruker Avance

DPX-300 spectrophotometer. FTIR spectra were recorded in a Perkin Elmer Spectrum 100 spectrometer.

2.2. Synthesis of carbon dots

Isoleucine surface functionalized carbon dot (CD_{iso}) was synthesized using reported protocol.^{9,37} Briefly, 1.1 g of L-isoleucine (14 mmol) was converted to its carboxylate salt by the addition of an equivalent amount of NaOH solution (2 mL). To this, 2 mL of citric acid solution (3 g, 14 mmol) was added by maintaining a 1 : 1 molar ratio. This water-soluble mixture was evaporated to dryness at 100 °C. The sticky mass was collected and dried in hot oven at 80 °C for 3 days. The solid was crushed into a fine powder and was heated in a furnace in air at 200 °C for 2 h in a porcelain crucible and then cooled to room temperature. The brownish-black product was extracted with 25 mL of water. The solution was centrifuged at 12 000 rpm for 30 min to discard the insoluble pellet. The supernatant was collected and dialyzed against water using a dialysis bag for further purification. The resultant solution was lyophilized to get the carbon dots. L-Valine and glycine surface functionalized carbon dots (CD_{val} and CD_{gly}) were synthesized using the similar protocol. The yield of the carbon dots was found to be around 60% in all cases.

2.3. Synthesis of phosphorous doped carbon dots

In case of the synthesis of P-doped isoleucine surface functionalized carbon dot (PCD_{iso}), 1.1 g of L-isoleucine (14 mmol) was converted to its carboxylate salt by the addition of an equivalent amount of NaOH solution (2 mL). To this, 2 mL of citric acid solution (3 g, 14 mmol) and 2 mL of NaH₂PO₄ solution (1.68 g, 14 mmol) were added by maintaining a 1 : 1 : 1 molar ratio. Then similar protocol was followed as for the synthesis of non-doped CDs. P-doped L-valine (PCD_{val}) and glycine (PCD_{gly}) functionalized CDs were synthesized by following the same process. A control experiment was done to carbonize citric acid in presence of NaH₂PO₄. The brown mass was insoluble in water. The yield of the phosphorous doped quantum dot was found to be around 65% in all cases.

2.4. Quantum yield measurement

Quantum yield of CDs and PCDs were measured using the reported protocols.²⁹ The absorbance of CDs and PCDs was measured using Perkin Elmer Lambda 25 spectrophotometer and the absorbance was restricted to less than 0.01. Integrated emission intensity at excitation maxima (340 nm for CDs and 370 nm for PCDs) of those solutions was measured using Varian Cary Eclipse luminescence spectrometer. To this end the quantum yield (QY) of the carbon dots was measured by the following equation:

$$Q = Q_{\text{st}}(I_{\text{sm}}/I_{\text{st}})(\text{OD}_{\text{st}}/\text{OD}_{\text{sm}})(\eta_{\text{sm}}^2/\eta_{\text{st}}^2)$$

where Q is the QY, I represents the measured integrated emission intensity at excitation maxima (340 nm for CDs and 370 nm for PCDs), η is the refractive index, and OD is the optical density measured on a UV-vis spectrophotometer, which was restricted

to less than 0.01. The subscript 'sm' indicates sample and the subscript 'st' stands for standard fluorophore of known fluorescence. Herein, we chose quinine sulfate dissolved in 0.1 M H_2SO_4 as a standard, whose QY is 0.54.

2.5. Characterization

Samples for transmission electron microscopy (TEM) were prepared by putting a drop of the prepared CD solutions on 300-mesh Cu-coated TEM grid and dried under vacuum for 4 h before taking the image. TEM images were taken on a JEOL JEM 2100F UHR microscope. For X-ray photoelectron spectroscopy (XPS) two drops of prepared CD solution was cast on a rectangular Cu plate and it was dried under vacuum for 8 h before the experiment which was performed using an Omicron (series 0571) X-ray photoelectron spectrometer. Energy dispersive X-ray (EDX) was performed on a Oxford make EXTREME INCA microscope and sample preparation was done like that of TEM. X-ray diffraction (XRD) spectra of powdered CDs were obtained on a Bruker D8 Advance diffractometer and the source was $\text{CuK}\alpha$ radiation ($\alpha = 0.15406$ nm) with a voltage 40 kV and current 30 mA.

2.6. Cell culture

HeLa cells were procured from NCCS, Pune and cultured in 10% FBS DMEM medium in presence of 100 mg L^{-1} streptomycin and 100 IU mL^{-1} penicillin. The cells were cultured in a 25 mL cell culture flask and kept at 37 °C in a humidified atmosphere of 5% CO_2 to about 70–80% confluence. Subculture was performed in every 2–3 days. The media was changed after 48–72 h. The adherent cells were detached from the surface of the culture flask by trypsinization. These cells were then used for cytotoxicity and bioimaging study.

2.7. MTT assay

Cell viability of the non-doped and P-doped CDs were assessed by the microculture MTT reduction assay by following the previously reported protocol.³⁸ In this assay, a soluble tetrazolium salt was converted to an insoluble colored product, formazan by mitochondrial dehydrogenase present in live cells. The amount of produced formazan was calculated spectrophotometrically after dissolution of the product in DMSO. The amount of formazan produced is proportional to the number of alive cells. The mammalian cells were seeded at a density of 15 000 cells per well in a 96-well microtiter plate 18–24 h before the assay. A stock solution of the CDs (5 mg mL^{-1}) was prepared in Milli-Q water. The concentration of CDs in the microtiter plate was varied from 100 to 800 $\mu\text{g mL}^{-1}$. The cells were incubated for 24 h at 37 °C under 5% CO_2 . The cells were further incubated for another 4 h in 15 μL MTT stock solution (5 mg mL^{-1}). The produced formazan was dissolved in DMSO and absorbance at 570 nm was measured using BioTek Elisa Reader. The number of surviving cells were expressed as percent viability = $(A_{570}(\text{treated cells}) - \text{background}) / (A_{570}(\text{untreated cells}) - \text{background}) \times 100$.

2.8. Bioimaging

HeLa cells were seeded at a density of 10 000 cells per well in a chamber slide 18–24 h before the assay. Cells were incubated with 200 $\mu\text{g mL}^{-1}$ of all the CD solutions for 6 h. Then the incubated cells were washed with phosphate-buffered saline (PBS), fixed with 4% paraformaldehyde for 30 min, mounted with 50% glycerol solution, and covered with cover slip to prepare the slide and kept for 24 h. Imaging was done in Olympus IX51 inverted microscope using an excitation filter BP 330–385 nm and a band absorbance filter covering wavelength below 405 nm for blue images and green images were obtained using the excitation filter BP 530–550 and a band absorbance filter covering wavelength below 570 nm. CCD exposure time during imaging was 400 ms and the microscopic object used was 40 \times UPlanFLN.

3. Results and discussion

3.1. Synthesis and characterization of carbon dots

Amino acid functionalized CDs (CD_{iso} , CD_{gly} , CD_{val}) were synthesized by thermal coupling between citric acid and different amino acids, L-isoleucine, L-valine and glycine, respectively (Fig. 1). Citric acid acted as the source of carbon core and Na-salts of amino acids were utilized for surface functionalities.^{36,37,39} In case of P-doped CDs, equivalent amount of NaH_2PO_4 was used along with the other precursor and the corresponding nanomaterials are defined as PCD_{iso} , PCD_{val} , and PCD_{gly} , (Fig. 1). The formation of amide bonds during thermal coupling between the citric acid derived CDs and amino acids was investigated using FTIR spectroscopy. In the

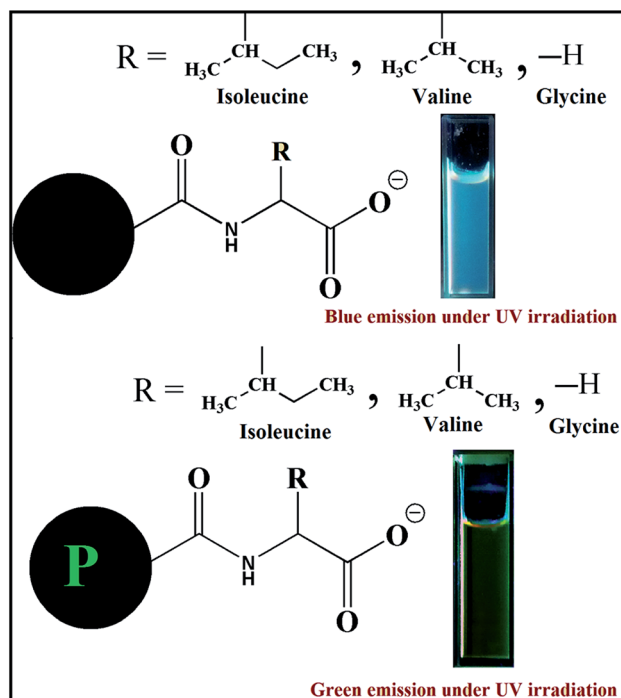


Fig. 1 Structure of the synthesized carbon dots (CDs) and phosphorous doped carbon dots (PCDs).

FTIR spectra of CD_{iso}, CD_{gly} and CD_{val} presence of a peak at 1700 cm⁻¹ confirmed the formation of amide bond (Fig. S1a, S1c and S1e, ESI†). Interestingly, in P-doped CDs (PCD_{iso}, PCD_{gly} and PCD_{val}), no change in FTIR spectra was observed which clearly indicates that even after phosphorous doping, the surface functionalization remains unaltered (Fig. S1b, S1d and S1f, ESI†).

Proton nuclear magnetic resonance (¹H NMR) analysis in D₂O was carried out for further establishment of surface functionalization of carbon dots. CD_{iso} showed peaks at δ 0.96 ppm and 1.0 ppm for two different -CH₃ groups. Broad peaks around 1.3 ppm is for -CH₂- and -CH- protons (Fig. S2a, ESI†). Similarly CD_{val} showed a broad peak around 1.0 ppm for six protons of two -CH₃ groups of valine, (Fig. S2c, ESI†). ¹H NMR spectra of CD_{iso} and CD_{val} showed a signal at 4.1 ppm, which corresponds to the asymmetric proton of isoleucine and valine, respectively. This characteristic peak indicates the presence of amino acid functionalization on the surface of CDs which resulted from the thermal coupling between citric acid and amino acids. Here too no change in the ¹H NMR spectrum pattern was observed for P-doped CDs (Fig. S2b, S2d and S2f, ESI†). This result further corroborates the fact that doped and non-doped CDs have similar surface functionalities.

The sizes of CDs and PCDs have been examined by taking their TEM images. The TEM images revealed that average size of doped and non-doped CDs are around 3–5 nm (Fig. 2). Zeta potential experiment indicates that all the CDs have anionic surface charge. The zeta potential (ζ) values of CD_{iso}, CD_{val} and CD_{gly} are -25.2, -18.9 and -22.0 mV, respectively. Similarly PCD_{iso}, PCD_{val}, and PCD_{gly} have ζ values of -14.7, -22.1 and -17.0 mV, respectively (Fig. S3, ESI†). These high ζ values support the aqueous solubility and stability of CDs and PCDs.

X-ray diffraction (XRD) experiment was carried out to investigate the structural changes of the CDs before and after phosphorous doping. XRD pattern of CD_{iso} showed a broad peak at 27° which indicates the presence of amorphous carbon (Fig. 3a). This peak corresponds to the diffraction of the (002) lattice of graphitic carbon.¹ It clearly indicates the graphitic structure of the carbon dot. Interestingly in case of PCD_{iso}, XRD pattern shows two distinct peaks at 18° and 30° which specified the change in the lattice structure of the carbon dot due to phosphorous doping (Fig. 3b). Similarly, CD_{gly} showed a single peak in XRD analysis indicating amorphous graphitic structure where as P-doped PCD_{gly} showed multiple peaks implying change in the lattice structure (Fig. 3c and d). PCD_{val} showed similar type of transformation in XRD pattern after phosphorous doping in CD_{val} like the previous two carbon dots (Fig. S4, ESI†). This splitting pattern of PCDs signified that some distortion took place in the doped carbon dot lattice. This structural deformation is due to doping of phosphorous, as no different synthetic phenomenon was applied except using the doping agent. High resolution TEM images also reveal the same observation. PCDs showed distinct lattice planes in its TEM images which is distinctly different from the TEM images of CDs (Fig. 2). This difference in TEM images indicate the change in morphology of the carbon dots after doping P which further support the result found in XRD analysis.

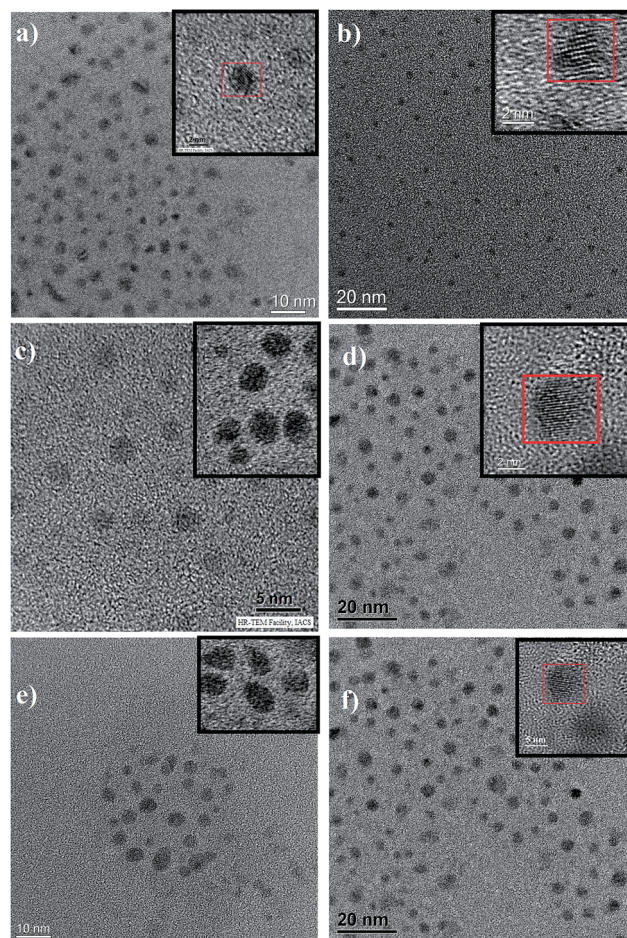


Fig. 2 TEM images of CDs and PCDs. (a) CD_{iso}, (b) PCD_{iso}, (c) CD_{gly}, (d) PCD_{gly}, (e) CD_{val}, (f) PCD_{val}. High resolution images of CDs and PCDs are given in inset.

Elemental analysis of the P-doped and non-doped CDs were investigated by XPS analysis. It showed the peaks at 285 eV, 418 eV and 532 eV that correspond to the C 1s, N 1s and O 1s, respectively for all CDs as the main elements present in CD_{iso}, CD_{gly} and CD_{val} are carbon, nitrogen and oxygen (Fig. 4a and c, S5a, ESI†).³¹ In case of PCD_{iso}, PCD_{gly} and PCD_{val}, in addition to the peaks for carbon, nitrogen and oxygen, two extra peaks were found at 134 eV and 191 eV which indicates the peaks correspond to 2p and 2s of phosphorous atom (P), respectively (Fig. 4b and d, S5b, ESI†).^{31,40} This characterization further established though little but successful doping of P in carbon dots. We also quantified the amount of phosphorous doped in the PCDs through EDX experiment. Around 16–18% phosphorous was found to be present in all the PCDs where as no notable peak for phosphorous was found in case of CDs in EDX analysis (Fig. S6, ESI†). This further proves the successful doping of phosphorous in carbon dots.

3.2. Photoluminescence of CDs and PCDs

All the synthesized CDs (both P-doped and non-doped) were found to be highly fluorescent. More importantly they showed excitation dependent emission property. Variation in the

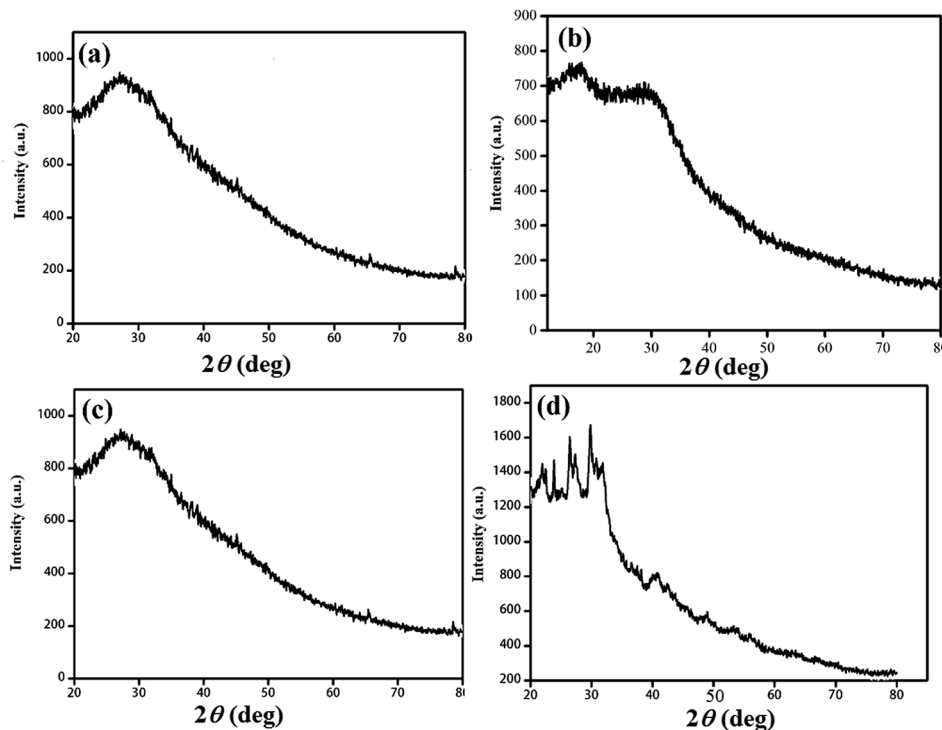


Fig. 3 XRD pattern of (a) CD_{iso} , (b) PCD_{iso} , (c) CD_{gly} , and (d) PCD_{gly} .

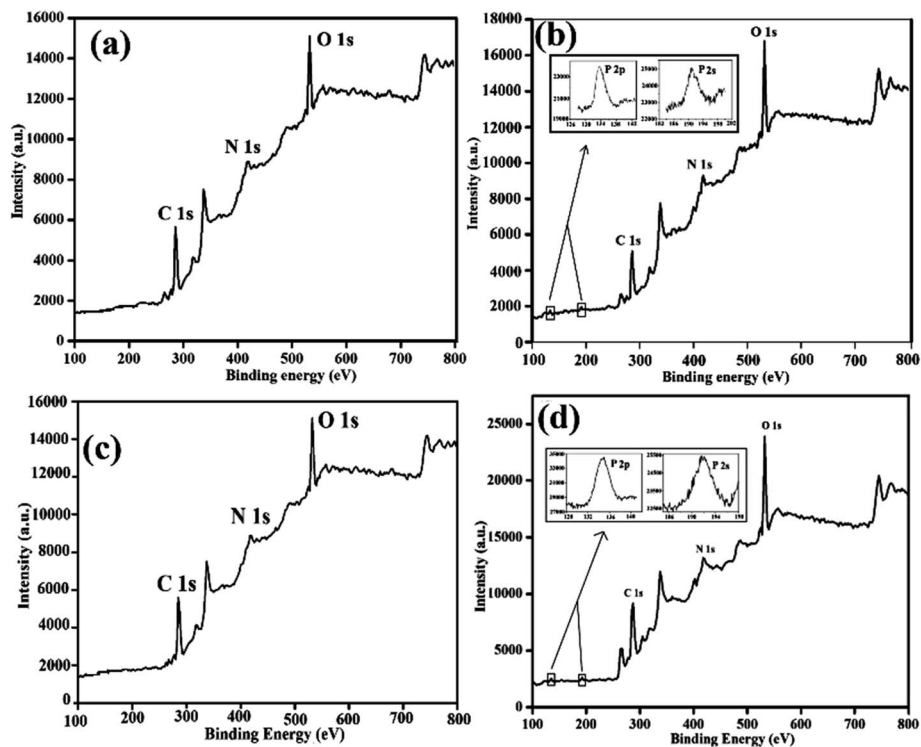


Fig. 4 XPS spectra of (a) CD_{iso} , (b) PCD_{iso} , (c) CD_{gly} , and (d) PCD_{gly} showing the presence of carbon (C), nitrogen (N), oxygen (O), and phosphorous (P).

excitation wavelength from 300 nm to 500 nm for CD_{iso} resulted in the red shifting of the emission peaks (Fig. 5a). PCD_{iso} also showed similar type of shift in its emission upon excitation at

different wavelength (Fig. 5b). XRD analysis showed the graphitic structure of the carbon dots which are due to the presence of huge amount of C=C (Fig. 3 and S4, ESI[†]).²⁹ This

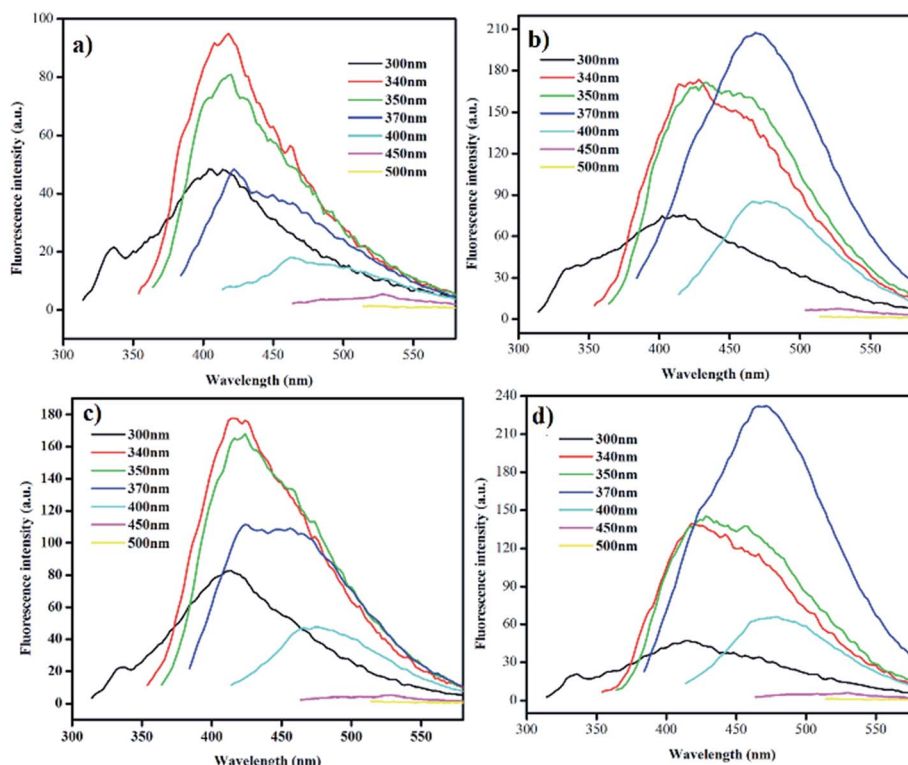


Fig. 5 Excitation wavelength dependent emission of (a) CD_{iso} , (b) PCD_{iso} , (c) CD_{val} and (d) PCD_{val} .

Table 1 Excitation and emission maxima of CDs and PCDs

Carbon dot	Excitation wavelength (nm)	Emission wavelength (nm)
CD_{iso}	340	420
PCD_{iso}	370	470
CD_{val}	340	420
PCD_{val}	370	470
CD_{gly}	340	420
PCD_{gly}	370	470

Table 2 Quantum yield of CDs and PCDs

Carbon dot	Quantum yield (%)
CD_{iso}	4.8
PCD_{iso}	15.2
CD_{val}	8.9
PCD_{val}	11.0
CD_{gly}	3.7
PCD_{gly}	19.7

indicates the presence of a series of emissive traps between π and π^* states of CDs.^{29,41} As a consequence when a certain excitation wavelength illuminates the carbon dots, a surface

energy trap dominates the emission.^{3,29} With variation in the excitation wavelength, different surface state emissive trap become dominant. Presumably because of this phenomenon CD_{iso} and PCD_{iso} showed excitation dependent emission

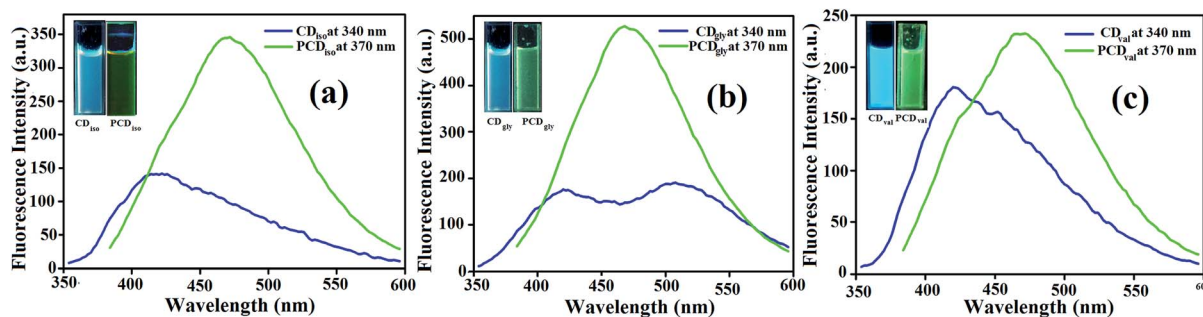


Fig. 6 Emission spectra of (a) CD and PCD from isoleucine, (b) CD and PCD from glycine, (c) CD and PCD from valine at their highest excitation wavelength. Inset: emission of the solutions under UV irradiation.

properties.^{41–43} Similar type of fluorescence behaviour was observed for CD_{val} and CD_{gly} and their P-doped PCD_{val} and PCD_{gly} (Fig. 5c and d, S7a and S7b, ESI†). Excitation maxima and the corresponding emission maxima of CDs and PCDs are provided in Table 1. It is evident that upon phosphorous doping, the excitation maxima red shifted from 340 nm to 370 nm as well as the emission maxima red shifted from 420 nm to 470 nm. This red shifting of the emission spectrum of carbon dots is probably because of the morphological changes in the PCDs compared to that of CDs. PCDs showed distinct lattice planes in its high resolution TEM images (inset, Fig. 2). This morphological change was also reflected in the XRD spectrum of CDs and PCDs. This red shifting in emission also got reflected in the corresponding emission colour of CDs and PCDs under UV light. CD_{iso}, CD_{val} and CD_{gly} showed intense blue colour upon UV light irradiation at 254 nm while the P-doped CDs like PCD_{iso}, PCD_{val} and PCD_{gly} exhibited intense green colour under the same conditions (Fig. 1 and 6). Interestingly, the fluorescence intensity of PCD_{iso}, PCD_{val}, and PCD_{gly} are many fold higher than that of the non-doped CD_{iso}, CD_{val} and CD_{gly} at their excitation maxima (Fig. 6). This fluorescence behaviour has also been observed in the respective quantum yield of CDs and PCDs. Quantum yield (QY) has been measured following the reported protocols considering quinine sulphate as the reference.²⁹ CD_{iso}, CD_{val} and CD_{gly} have QY of 4.8%, 8.9% and 3.7%, respectively while the PCD_{iso}, PCD_{val}, and PCD_{gly} have QY of 15.2%, 11.0% and 19.7%, respectively (Table 2). Increment in fluorescence intensity as well as QY of PCDs is due to the increase in sp² isolated clusters.⁴⁴ Presumably, coexistence of defect sites and isolated sp² carbon clusters efficiently increase the band gap in UV-vis region and hence given rise to stronger fluorescence than single sp² carbon.^{32,41,44,45} Thus blue to green spectral transition with high QY was obtained by simple doping of phosphorus to the carbon dots.

3.3. Cell viability

The prospective application of these fluorescent CDs and PCDs in biology is dependent on its toxicity towards eukaryotic

cells. To this end, initially we investigated the photostability of the doped and non-doped CDs by exposing the aqueous solution of carbon dots under UV irradiation (wavelength 365 nm, power 12 watt).⁴⁶ Interestingly, the CDs and PCDs solutions didn't show any photobleaching and fluorescence remained unchanged even after 200 min of UV exposure (Fig. S8, ESI†). To ensure their cytocompatibility, MTT assay was performed first with all the synthesized CDs with a concentration range of 100–800 μg mL⁻¹ and it was found that 80% cells were alive with CD_{gly} whereas more than 90% cells were alive with CD_{iso} and CD_{val} after 24 h of incubation (Fig. 7). Alternatively with all the P-doped CDs more than 90% cells were alive with all the PCDs over the same concentration range and over same time period. Thus it can be concluded that all the CDs and PCDs were sufficiently biocompatible to be utilized for biological purposes.

3.4. Bioimaging

High cell viability and unwavering fluorescence are the primary requisites for CDs to be used as bioimaging probe. HeLa cells were incubated with 200 μg mL⁻¹ of the CDs solutions for 6 h. Depending on the emission properties of P-doped and non-doped CDs, different excitations wavelength were applied to take the image of the CD labeled cells. Cells labeled with non-doped carbon dots CD_{iso}, CD_{val} and CD_{gly} showed bright blue emission (Fig. 8) which corroborates with the fluorescence emission maxima of CDs at 420 nm. On the other hand with PCDs having emission maxima at 470 nm (PCD_{iso}, PCD_{val} and PCD_{gly}) cells illuminated with green fluorescence (Fig. 8). Excellent and divergent application of prepared CDs and PCDs as cell labeling probe was noted. Small sized negatively charged amino acid functionalized CDs exhibited bright blue and green cellular images indicating their successful internalization within the cells. Naturally occurring biofriendly precursor amino acids functionalization and small size of the CDs probably resulted in high cytocompatibility and smooth uptake across the membrane by the cells. Thus by simple doping simultaneous blue and green biocompatible fluorescent probes

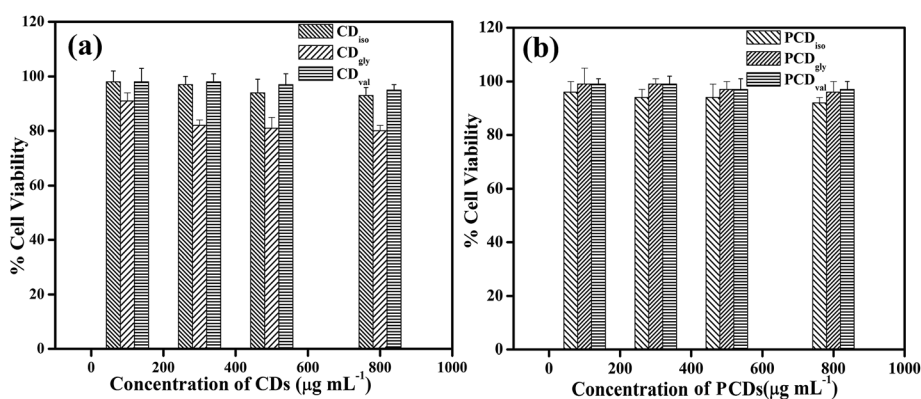


Fig. 7 Percentage cell viability of HeLa cells incubated with varying concentrations of (a) CDs and (b) PCDs after 24 h incubation. The experimental errors were in the range of 3–5% in triplicate experiments.

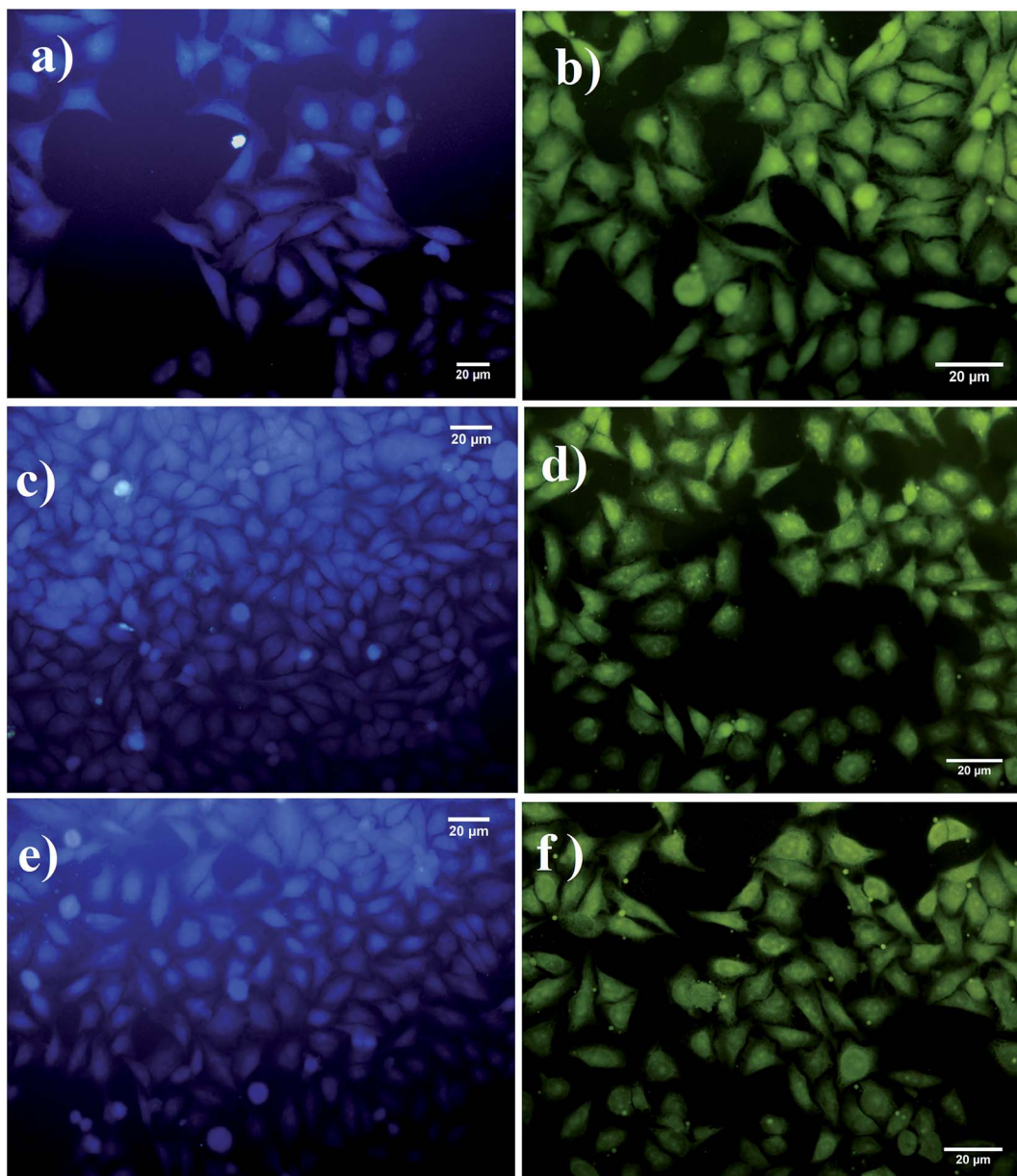


Fig. 8 Fluorescence microscopic images of HeLa cells upon incubation with CD_{iso} , CD_{gly} and CD_{val} (a, c and e) and with PCD_{iso} , PCD_{gly} and PCD_{val} (b, d and f), respectively after 6 h of incubation.

were developed which holds its promise to be used as potential bioimaging probe.

4. Conclusion

In summary, L-isoleucine, L-valine and glycine functionalized fluorescent CDs were synthesized using citric acid as carbon core. These CDs were found to be blue emitting. Interestingly P-doping had a pronounced effect on photoluminescence property of CDs. In case of PCDs, quantum yield had improved compared to CDs due to phosphorous doping. The as-prepared CDs and PCDs had definite surface chemistry, a high yield and good water solubility. They were also found to be biocompatible and were devoid of any photobleaching property. Thus these

doped and non-doped CDs were used as both blue and green fluorescent optical imaging probe to label HeLa cells. Simple doping resulted in diversely applicable, low toxic fluorescent probes for optical imaging both *in vitro* and *in vivo* studies.

Acknowledgements

P. K. D. is thankful to Department of Science and Technology, India (SR/S1/OC-25/2011) for financial assistance. S. S. acknowledges DST, India for Research Fellowship. K. D. and M. G. acknowledge CSIR, India for Research Fellowships. The authors are thankful to DST Unit of Nanoscience, IACS for the XPS facility.

References

- J. Jiang, Y. He, S. Li and H. Cui, *Chem. Commun.*, 2012, **48**, 9634–9636.
- H. Liu, T. Ye and C. Mao, *Angew. Chem., Int. Ed.*, 2007, **46**, 6473–6475.
- Y. P. Sun, B. Zhou, Y. Lin, W. Wang, K. A. S. Fernando, P. Pathak, M. J. Mezziani, B. A. Harruff, X. Wang, H. Wang, P. G. Luo, H. Yang, M. E. Kose, B. Chen, L. M. Veca and S. Y. Xie, *J. Am. Chem. Soc.*, 2006, **128**, 7756–7757.
- S. Zhu, Q. Meng, L. Wang, J. Zhang, Y. Song, H. Jin, K. Zhang, H. Sun, H. Wang and B. Yang, *Angew. Chem., Int. Ed.*, 2013, **52**, 3953–3957.
- H. Huang, C. Li, S. Zhu, H. Wang, C. Chen, Z. Wang, T. Bai, Z. Shi and S. Feng, *Langmuir*, 2014, **30**, 13542–13548.
- G. H. G. Ahmed, R. B. Laiño, J. A. G. Calzón and M. E. D. García, *Talanta*, 2015, **132**, 252–257.
- S. T. Yang, L. Cao, P. G. Luo, F. Lu, X. Wang, H. Wang, M. J. Mezziani, Y. Liu, G. Qi and Y. P. Sun, *J. Am. Chem. Soc.*, 2009, **131**, 11308–11309.
- Q. Wang, X. Huang, Y. Long, X. Wang, H. Zhang, R. Zhu, L. Liang, P. Teng and H. Zheng, *Carbon*, 2013, **59**, 192–199.
- S. Maiti, K. Das and P. K. Das, *Chem. Commun.*, 2013, **49**, 8851–8853.
- M. Lan, J. Zhang, Y. S. Chui, H. Wang, Q. Yang, X. Zhu, H. Wei, W. Liu, J. Ge, P. Wang, X. Chen, C. S. Lee and W. J. Zhang, *J. Mater. Chem. B*, 2015, **3**, 127–134.
- M. Lan, J. Zhang, Y. S. Chui, P. Wang, X. Chen, C. S. Lee, H. L. Kwong and W. Zhang, *ACS Appl. Mater. Interfaces*, 2014, **6**, 21270–21278.
- S. N. Baker and G. A. Baker, *Angew. Chem., Int. Ed.*, 2010, **49**, 6726–6744.
- L. Wang, Y. Yin, A. Jain and H. S. Zhou, *Langmuir*, 2014, **30**, 14270–14275.
- H. Huang, J. J. Lv, D. L. Zhou, N. Bao, Y. Xu, A. J. Wang and J. J. Feng, *RSC Adv.*, 2013, **3**, 21691–21696.
- L. Zhou, Z. Li, Z. Liu, J. Ren and X. Qu, *Langmuir*, 2013, **29**, 6396–6403.
- X. Wang, L. Cao, S. T. Yang, F. Lu, M. J. Mezziani, L. Tian, K. W. Sun, M. A. Bloodgood and Y. P. Sun, *Angew. Chem., Int. Ed.*, 2010, **49**, 5310–5314.
- S. L. Hu, K. Y. Niu, J. Sun, J. Yang, N. Q. Zhao and X. W. Du, *J. Mater. Chem.*, 2009, **19**, 484–488.
- S. Zhu, Y. Song, X. Zhao, J. Shao, J. Zhang and B. Yang, *Nano Res.*, 2015, **8**, 355–381.
- H. Yu, Y. Zhao, C. Zhou, L. Shang, Y. Peng, Y. Cao, L. Z. Wu, C. H. Tung and T. Zhang, *J. Mater. Chem. A*, 2014, **2**, 3344–3351.
- X. Xu, R. Ray, Y. Gu, H. J. Ploehn, L. Gearheart, K. Raker and W. A. Scrivens, *J. Am. Chem. Soc.*, 2004, **126**, 12736–12737.
- P. C. Hsu and H. T. Chang, *Chem. Commun.*, 2012, **48**, 3984–3986.
- Y. Dong, H. Pang, H. B. Yang, C. Guo, J. Shao, Y. Chi, C. M. Li and T. Yu, *Angew. Chem., Int. Ed.*, 2013, **52**, 7800–7804.
- W. Li, Z. Zhang, B. Kong, S. Feng, J. Wang, L. Wang, J. Yang, F. Zhang, P. Wu and D. Zhao, *Angew. Chem., Int. Ed.*, 2013, **52**, 8151–8155.
- H. G. Baldovi, S. Valencia, M. Alvaro, A. M. Asirib and H. Garcia, *Nanoscale*, 2015, **7**, 1744–1752.
- L. Tang, R. Ji, X. Cao, J. Lin, H. Jiang, X. Li, K. S. Teng, C. M. Luk, S. Zeng, J. Hao and S. P. Lau, *ACS Nano*, 2012, **6**, 5102–5110.
- H. Li, X. He, Y. Liu, H. Huang, S. Lian, S. T. Lee and Z. Kang, *Carbon*, 2011, **49**, 605–609.
- S. Zhu, Q. Meng, L. Wang, J. Zhang, Y. Song, H. Jin, K. Zhang, H. Sun, H. Wang and B. Yang, *Angew. Chem., Int. Ed.*, 2013, **52**, 3953–3957.
- C. Liu, P. Zhang, F. Tian, W. Li, F. Li and W. Liu, *J. Mater. Chem.*, 2011, **21**, 13163–13167.
- S. Sahu, B. Behera, T. K. Maiti and S. Mohapatra, *Chem. Commun.*, 2012, **48**, 8835–8837.
- M. Sevilla and A. B. Fuertes, *Chem.–Eur. J.*, 2009, **15**, 4195–4203.
- S. K. Bhunia, N. Pradhan and N. R. Jana, *ACS Appl. Mater. Interfaces*, 2014, **6**, 7672–7679.
- M. K. Barman, B. Jana, S. Bhattacharyya and A. Patra, *J. Phys. Chem. C*, 2014, **118**, 20034–20041.
- S. K. Bhunia, A. Saha, A. R. Maity, S. C. Ray and N. R. Jana, *Sci. Rep.*, 2013, **3**, 1473–1479.
- C. Wang, D. Sun, K. Zhuo, H. Zhang and J. Wang, *RSC Adv.*, 2014, **4**, 54060–54065.
- K. Das, S. Maiti and P. K. Das, *Langmuir*, 2014, **30**, 2448–2459.
- A. B. Bourlino, A. Stassinopoulos, D. Anglos, R. Zboril, M. Karakassides and E. P. Giannelis, *Small*, 2008, **4**, 455–458.
- A. B. Bourlino, A. Stassinopoulos, D. Anglos, R. Zboril, V. Georgakilas and E. P. Giannelis, *Chem. Mater.*, 2008, **20**, 4539–4541.
- M. B. Hansen, S. E. Nielsen and K. Berg, *J. Immunol. Methods*, 1989, **119**, 203–210.
- J. Moskon, R. Dominko, M. Gaberscek, R. Cerc-Korošec and J. Jamnik, *J. Electrochem. Soc.*, 2006, **153**, A1805–A1811.
- J. Zhou, X. Shan, J. Ma, Y. Gu, Z. Qian, J. Chen and H. Feng, *RSC Adv.*, 2014, **4**, 5465–5468.
- V. N. Mochalin and Y. Gogotsi, *J. Am. Chem. Soc.*, 2009, **131**, 4594–4595.
- D. V. Melnikov and J. R. Chelikowsky, *Phys. Rev. Lett.*, 2004, **92**, 046802.
- Y. Xu, M. Wu, Y. Liu, X. Z. Feng, X. B. Yin, X. W. He and Y. K. Zhang, *Chem.–Eur. J.*, 2013, **19**, 2276–2283.
- J. Peng, W. Gao, B. K. Gupta, Z. Liu, R. R. Aburto, L. Ge, L. Song, L. B. Alemany, X. Zhan, G. Gao, S. A. Vithayathil, B. A. Kaiparettu, A. A. Marti, T. Hayashi, J. J. Zhu and P. M. Ajayan, *Nano Lett.*, 2012, **12**, 844–849.
- Z. Qian, J. Zhou, J. Ma, X. Shan, C. Chen, J. Chen and H. Feng, *J. Mater. Chem. C*, 2013, **1**, 307–314.
- C. Huang, Q. Yin, W. Zhu, Y. Yang, X. Wang, X. Qian and Y. Xu, *Angew. Chem., Int. Ed.*, 2011, **50**, 7551–7556.